

# Determination of Temperature Gradient and Spectrum in the Mold's Core and Wall by Solving the Differential Equations Using Wolfram Mathematica Software

*Luu Thuy Chung*<sup>1,2\*</sup>, *Dinh Thanh Binh*<sup>1,3</sup>, *Nguyen Thi Phuong Mai*<sup>1</sup>, *Pham Hong Tuan*<sup>4</sup>

<sup>1</sup> Hanoi University of Science and Technology - No. 1, Dai Co Viet Str., Hai Ba Trung, Ha Noi, Viet Nam

<sup>2</sup> Vinh University of Technology Education, Nguyen Viet Xuan Str., Vinh, Nghe An, Viet Nam

<sup>3</sup> Defense industrial college, Thanh Vinh, Phu Tho, Phu Tho, Viet Nam

<sup>4</sup> National Center for Technological Progress, C6-Thanh Xuan Bac, Thanh Xuan, Ha Noi, Viet Nam

Received: December 08, 2017; Accepted: June 24, 2019

## Abstract

Using of mathematical tools to calculate, simulate the technical problems is widely used by many researchers. This study was developed based on the Wolfram Mathematica software to determine the temperature spectral and temperature gradient transmittance in the mold's wall and core, in order to determine the influence of the material thermal conductivity to the mold temperature gradient, as well as evaluating the effect of changing the position of the mold surface to the thermal gradient in the mold. The calculations demonstrated that the increasing of the coefficient of thermal conductivity of the mold material would reduce the temperature gradient of the mold, and the mold walls were identified to have higher thermal gradient than in the mold's core that were in similar working conditions. The experiments had also shown that TiN and CrN had the same temperature and temperature gradient spectrums as the SKD61, but the gradient values on their surfaces were higher than those of SKD61 and the slopes were higher, too.

Keywords: Thermal differential equation, temperature spectrum, thermal gradient spectrum

## 1. Introduction

Using mathematical tools to solve the heat transfer problem was investigated in the field of mathematics while physics or informatics studies the ability of software to solve the problem of heat transfer by software [1]. In the field of foundry research, the author [2] has given the mathematical solution to the problem of heat transfer in the mold in a static state by using error function. Some other researchers used simulation softwares to simulate the thermal processes in the mold [3, 4].

Thermal fatigue was one of the major failures of in high pressure die casting (HPDC) mold, which was a widespread and unavoidable phenomenon [5-9]. Numerous researches had shown that the thermal stresses occur in the HPDC mold due to heat gradients and temperature raise in the mold. The temperature of mold was always increased due to the contact of the mold surface and the molten metal, so the stress component due to the temperature rising was an inevitable factor component. This study focuses on the influence of the physical properties of the material on the thermal gradients of the die

casting mold and on the mold surface characteristics in the mold to the thermal gradient.

In temperature field of the mold, due to the difference in temperature between the locations in the wall, according to the laws of thermal expansion of the material, the mold material expanded unevenly between the positions, which caused stress in the mold. The stress produced in a tiny part of mold was proportional to the difference in elongation of the edges following  $a$   $x$  direction, thus the thermal gradient stress is:

$$\sigma = E.\Delta\varepsilon = E.\frac{\alpha.\text{grad}_x u.dx}{dx} = E.\alpha.\text{grad}_x u \quad (1)$$

The equation (1) shows that the temperature and gradient of mold greatly affect to the stresses at different positions of the mold during processing. Further studies determined the thermal together with gradient spectrums of the mold that occur to further clarify the thermal stresses of the mold. Considering two models of heat transfer: through flat wall (equivalent to heat transfer through mold walls) and into square root (equivalent to thermal transfer of core).

Thermal equation for heat transfer (Fourier equations) [10]:

\* Corresponding author: Tel.: (+84) 98.234.1350  
Email: lthuychung@gmail.com

$$\frac{\partial u}{\partial t} = -a \left( \frac{\partial^2 u}{\partial x^2} + \frac{\partial^2 u}{\partial y^2} + \frac{\partial^2 u}{\partial z^2} \right) \quad (2)$$

Here,  $u$  is the temperature;  $t$  is time and  $x, y, z$  are coordinates with  $a = \frac{\lambda}{c_p \cdot \rho}$  determinate by  $\lambda$  - The specific heat of the material,  $\rho$  - Specific mass of the material. The values  $\lambda, c_p, \rho$  for some materials [11] related with this study were shown in Table 1.

**Table 1.** Specific heat ( $C$ ), density ( $\rho$ ), heat transfer coefficient ( $\lambda$ ) and thermal conductivity ( $a$ )

Material	Specific heat, $C$ (kJ/kg.K)	Density, $\rho$ (g/cm <sup>3</sup> )	Heat transfer coefficient, $\lambda$ (W/m.K)	Thermal conductivity, $a$ (mm <sup>2</sup> /s)
Steel	0.45-0.50	7.8	50	14.24-12.82
SKD61	0.46-0.59	7.6-7.8	24.3-27.5	≈6.78 (100-300 °C)
TiN	0.78	5.22	19	4.67
CrN	0.73	6.14	12	2.68
W	0.14	19.3	173	64.03

Initial condition of the differential equation is the mold temperature at the start state, choosing ambient temperature. In this case the ambient temperature is 22 °C.

The boundary conditions of the differential equation were the surface temperature of the mold. In the case of wall part, the surface of the mold is the surface of the molten liquid contact, with a thermal cycle described as curve 1 (Fig.1a), the outer surface is a cyclic air contact surface as shown by curve 2 (Fig.1a), in the case of the core of the mold, all the faces of the mold part are cast metal contact surfaces, and all of them use the spectral 1 in Fig.1a. In this case, Fig.1a is a graph of mold temperature from the document of casting machines (company Z117 - Ministry of Defense). These curves took similar forms to the results of other researches in [3, 12, 13].

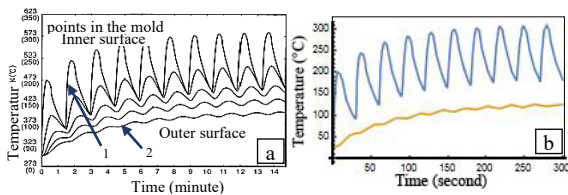


**Fig.1.** Temperature variation at points in the mold over time: (a) real charts and (b) simulation chart

## 2. Numerical Modeling

### 2.1. Setup the differential functions

There are 2 main cases of heat transfer on the mold. Heat transfer through the wall and heat transfer into the core.

In the first case, in order to simply the problem, considering the remaining 2 other directions of the wall are large enough, the problem can be seen as one direction heat transfer. In this case, there is no  $y$  and  $z$  components in differential equation, so equation (3) is the form of equation (2) in this case. The equation can be shown as equation (4) in the software.

$$\frac{\partial u}{\partial t} = -a \frac{\partial^2 u}{\partial x^2} \quad (3)$$

$$D[u[x,t],t] == a * D[u[x,t],x,x] \quad (4)$$

For the second case of heat transfer in the mold: When heat is transferred to the square core, the  $z$  component is not involved in the differential equation, in this case the equation (2) is expressed as equation (5) and (6).

$$\frac{\partial u}{\partial t} = -a \left( \frac{\partial^2 u}{\partial x^2} + \frac{\partial^2 u}{\partial y^2} \right) \quad (5)$$

$$D[u[x,y,t],t] == a * (D[u[x,y,t],x,x] + D[u[x,y,t],y,y]) \quad (6)$$

The value of thermal conductivity ( $a$ ) in the functions (3, 4, 5, 6) depends on specifically material as shown in Table 1, in these experiments, we use 4 “ $a$ ” values of mold material SKD61, hard coating material TiN, CrN and W.

### 2.2. Initial conditions and boundary conditions

As indicating, the initial condition of the problem is that the mold temperature at the starting time of the process is the ambient temperature. This initial condition is described as follows:

$$u[x,0] == 22 \quad (7)$$

$$uu[x,y,0] == 22 \quad (8)$$

In these cases, we use Dirichlet Boundary Condition by describing the mold surfaces’ temperatures. To simply describe the thermal of mold surface in the differential equation, the charts (shown in Fig.1a) is rescaled, divided into sort parts, linearized and define by the form of function as Eq. 9.

$$u_0 = \begin{cases} u_{01} + u'_{01} t & 0 \leq t \leq t_{01} \\ u_{02} + u'_{02} t & t_{01} < t \leq t_{02} \\ \dots & \dots \\ u_{0n} + u'_{0n} t & t_{0n-1} < t \leq t_{0n} \end{cases} \quad (9)$$

Two functions that defined by the Mathematica software’s Function Piecewise ndbmkhun[t] and ndmnkhun[t] have been created. Fig.1b shows the charts of the functions ndbmkhun[t] and ndmnkhun[t] in the software. Comparison of Fig.1a and Fig.1b shows that the charts of the functions are

similar to the origin chart, so we can use these functions in models.

**2.3. Solving the models**

To solve the differential equations (4), (6) with the initial conditions (7), (8) and the boundary conditions as  $ndbmkhun[t]$  and  $ndmnkhun[t]$  functions, we use the NDSolve function. The full setup functions are shown as equation (10) and (11).

$$nhiet=NDSolve\{D[u[x,t],t]==a*D[u[x,t],x,x], u[x,0]==22,u[0,t]==ndbmkhun[t], u[50,t]==ndmnkhun[t],u,\{x,0,50\},\{t,0,300\}\} \tag{10}$$

$$nhiet2=NDSolve\{D[uu[x,y,t],t]==a*(D[uu[x,y,t],x,x]+D[uu[x,y,t],y,y]),uu[x,y,0]==22, uu[0,y,t]==ndbmkhun[t],uu[50,y,t]==ndbmkhun[t],uu[x,0,t]==ndbmkhun[t],uu[x,50,t]==ndbmkhun[t],uu,\{x,0,50\},\{y,0,50\},\{t,0,300\}\} \tag{11}$$

The equation (10) is used to solve the temperature function  $u[x,t]$  in the case of 1D thermal transfer. The equation (11) is used to solve the temperature function  $uu[x,y,t]$  in the case of 2D thermal transfer.

The thermal gradient in the material is illustrated by taking the derivative of the temperature function  $u[x,t]$  or  $uu[x,y,t]$  along the x-axis with the function  $D[u[x,t],x]$  or  $D[uu[x,y,t],x]$ .

**3. Discussions**

Usage of the Plot and Plot3D function for representing the interpolation values of the heat transfer functions in the 2 and 3-dimensional charts to fully observe the temperature fields and the temperature gradient distribution field in various materials or shapes.

**3.1. Effect of thermal conductivity to thermal gradient**

The equation (10) has been solved with different values of “a” to evaluate the effect of the thermal conductivity “a” on the thermal spectrum and thermal gradient spectrum. In Fig.2, 3, 4, the temperature and thermal gradient changed for cases  $a = 2.68$ ,  $a = 4.67$  (low enough “a” values),  $a = 6.78$  (coefficient of thermal conductivity of the SKD61 mold), and  $a = 64.03$  (high enough “a” value).

As the thermal conductivity increases from 2.68 to 4.67, 6.78 and 64.03, the faster the material reached the stable state (from the 10<sup>th</sup> cycle to the 7<sup>th</sup> cycle) as shown in Fig.2. Fig.2 and 3 also showed that, as the thermal conductivity increased, the influence of thermal oscillations was deeper (from less than 10 mm to greater than 40 mm). Temperature variations at points in the mold wall are consistent with the results in the previous study [3]. Fig.4

illustrates that the thermal gradients reached the highest value on the mold surface, which was achieved at 275.7s (or 5.7s of the cycle). Fig.5 shows the thermal gradient spectrum of the mold in a section along the thermal transmission direction also recognizes the highest gradient values on the mold surface. These maximums depended on the thermal conductivity of the material. The lower thermal conductivity of material is (CrN,  $a = 2.68$ ; TiN,  $a = 4.67$ ), the higher gradient value had achieved on the surface (about 29 °C/mm and 22°C/mm). On the contrary, the better heat conducting material (W,  $a = 64.03$ ) had the lower gradient value on the mold surface (about 7.5°C/mm).

The thermal gradients dropped drastically near to the surface and then slowed down further when deeper. The thermal gradients on the surfaces of the less heat conduction materials (CrN, TiN) decreased faster (slope of CrN is 6.6°C/mm<sup>2</sup> at the surface, 2.4°C/mm<sup>2</sup> at 5mm depth, the slope of TiN decreased from 3.75°C/mm<sup>2</sup> on the surface to 1.9°C/mm<sup>2</sup> at 5mm depth) than the better thermal conductivity material’s (W has 0.28°C/mm<sup>2</sup> on the surface and 0.24°C/mm<sup>2</sup> at a depth of 5mm) as shown in Fig.5.

Fig.4c and 5c presented that SKD61 had a gradient value up to 18,383 °C/mm on the surface at 275.7s.

The thermal conductivities of the two coating materials in these simulations were lower than those of SKD61 and close to the coefficient of thermal conductivity of SKD61. The charts of these two materials are similar to those of SKD61 but the maximum value (on the surface) of the highest thermal gradient and the slope of the charts is higher than the charts of SKD61 (2.54°C/mm<sup>2</sup> on the surface and 1.54°C/mm<sup>2</sup> at the depth of 5mm) as shown in Fig.5.

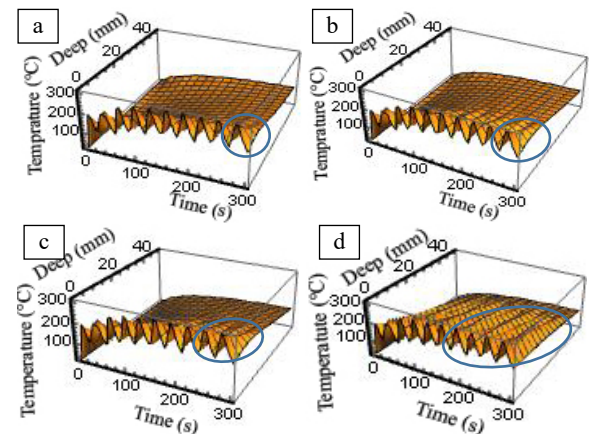


**Fig. 2.** Temperature spectrums in first 10 cycles by materials: (a) CrN ( $a = 2.68$ ); (b) TiN ( $a = 4.67$ ); (c) SKD61 ( $a = 6.78$ ) and (d) W ( $a = 64.03$ )

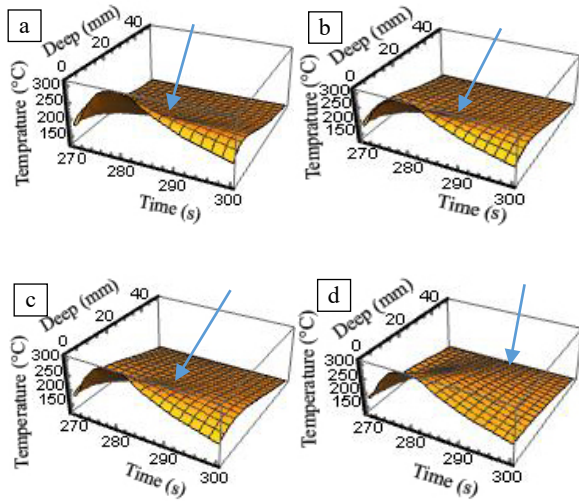


Fig. 3. Temperature spectrums in the 10<sup>th</sup> cycle by materials: (a) CrN; (b) TiN; (c) SKD61 and (d) W

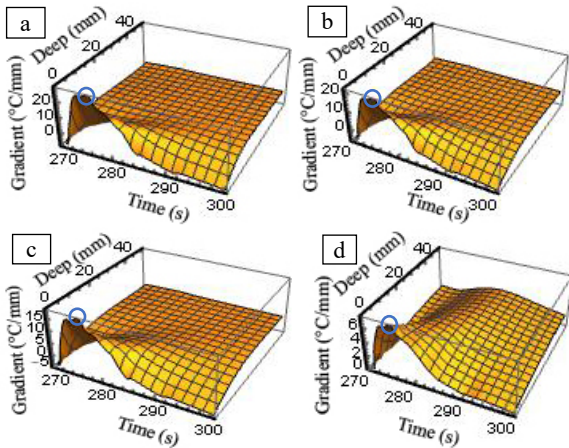


Fig. 4. Thermal gradient spectrums in the 10<sup>th</sup> cycle by materials: (a) CrN; (b) TiN; (c) SKD61 and (d) W

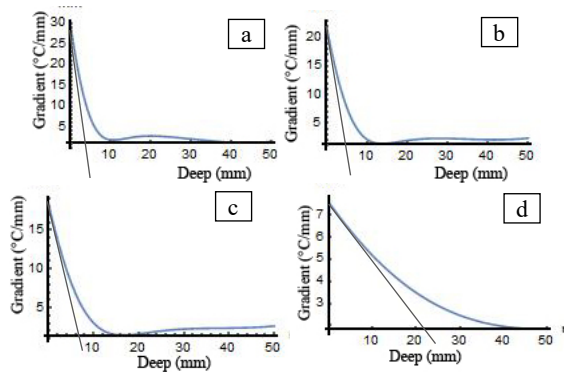


Fig. 5. Thermal gradient spectrums in a section along the thermal transmission at the time of 275.7s by materials: (a) CrN; (b) TiN; (c) SKD61 and (d) W

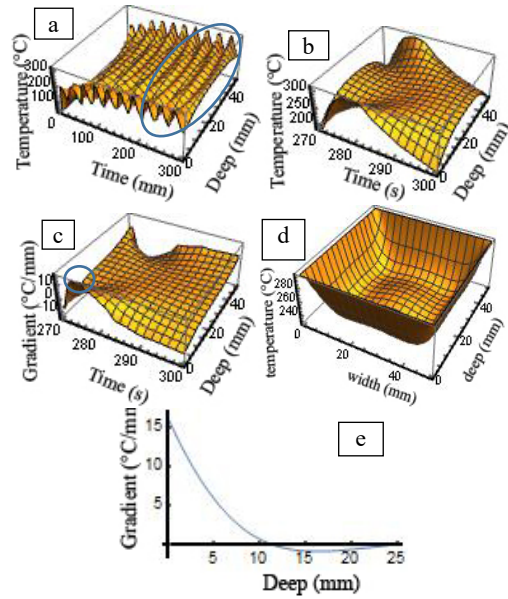


Fig. 6. Thermal spectrums in the (square) SKD61 core: (a) temperature spectrum in the first 10 cycles; (b) temperature spectrum in the 10<sup>th</sup> cycle; (c) thermal gradient spectrum in the 10<sup>th</sup> cycle; (d) temperature in a cross section at 275.74s; (e) thermal gradient spectrum along the section at 275.74s

### 3.2. Effect of position in the mold to the temperature field

Fig.6 shows the results of the thermal process simulation taking place in the SKD61 core by solving the differential equation (5) with the boundary conditions ndbmkhuon as the equation (11). Fig.6d shows that the longitudinal section at the center of the core resulted in the highest thermal gradient. The maximum value of the thermal gradient appeared at 275.74s on the mold surface (Fig.6c). In comparison with the wall case (Fig.2c), Fig.6a shows that in the case of a mold core, thermal processes were rapidly gaining stability (from the eighth cycle). In contrast to wall case (Fig.2c and 3c), Fig.6a and 6b showed that the heat in the core affects to the entire cross section of the core.

Fig.6c and 6e showed that the thermal gradient reached the maximum value on the mold surface at 16°C/mm. Fig.6e also showed that the slope of the heat gradient graph in the case of the core was also smaller than that of the wall at the near surface (2.8°C/mm<sup>2</sup> on the surface and 1.5°C/mm<sup>2</sup> at 5mm depth).

### 4. Conclusion

The thermal conductivity factor had influence on the spectral shape and the maximum gradient value on the surface. Thermal conductivity of CrN as 2.68, which was the lowest value of these simulations

in our researched materials. Simulation illustrated that the gradient of CrN was the highest value (about  $29^{\circ}\text{C}/\text{mm}$ ) by contrast to W ( $a = 64.03$ ) with the gradient value of  $7.5^{\circ}\text{C}/\text{mm}$ .

The thermal conductivity of the cores quickly attained stability (at the eighth cycle toward) over the walls (at the tenth cycle toward). After achieving stability, each cycle time  $\sim 5.7\text{s}$  would be the time when the mold surface temperature and the thermal gradient on the mold surface was highest. In general, the thermal gradient of the mold core ( $16^{\circ}\text{C}/\text{mm}$ ) was smaller than that of the wall profile ( $18,383^{\circ}\text{C}/\text{mm}$ ).

Gradients dropped very fast ( $6.6^{\circ}\text{C}/\text{mm}^2$  – CrN,  $3.75^{\circ}\text{C}/\text{mm}^2$  – TiN,  $2.55^{\circ}\text{C}/\text{mm}^2$  – SKD61) on the surface, then changed slowly in deep points ( $2.4^{\circ}\text{C}/\text{mm}^2$  – CrN,  $1.9^{\circ}\text{C}/\text{mm}^2$  – TiN,  $1.75^{\circ}\text{C}/\text{mm}^2$  – SKD61 at 5mm) of the mold.

The thermal stresses of coating materials were higher than that value of SKD61, the coating layer had great thermal gradient, so the mold substrate lifetime was extended as shown in [2].

The results of temperature evolution calculations are consistent with previous study [3].

## References

- [1] Huỳnh Thị Thuý Phượng; Ứng dụng phần mềm Mathematica cho lời giải bài toán truyền nhiệt; luận văn thạc sỹ khoa học, ĐH Đà Nẵng, 2012.
- [2] Nguyễn Hữu Dũng; Các phương pháp đúc đặc biệt; NXB Khoa học kỹ thuật, 2006.
- [3] A. Srivastava, V. Joshi, R. Shivpuri; Computer modeling and prediction of thermal fatigue cracking in die-casting tooling; *Wear* 256 (2004) 38–43.
- [4] Yi Han, Xiao-Bo Zhang, Enlin Yu, Lei Sun, Ying Gao; Numerical analysis of temperature field and structure field in horizontal continuous casting process for copper pipes; *International Journal of Heat and Mass Transfer* 115 (2017) 294–306.
- [5] Amit Srivastava, Vivek Joshi, Rajiv Shivpuri, Rabi Bhattacharya, Satish Dixit; A multilayer coating architecture to reduce heat checking of die surfaces; *Surface and Coatings Technology* 163 –164 (2003) 631–636.
- [6] Changrong Chen, Yan Wang, Hengan Ou, Yueh-Jaw Lin; Energy-based approach to thermal fatigue life of tool steels for die casting dies; *International Journal of Fatigue* 92 (2016) 166–178.
- [7] S. Jhavar, C.P. Paul, N.K. Jain; Causes of failure and repairing options for dies and molds: A review; *Engineering Failure Analysis* 34 (2013) 519–535
- [8] V. Nunes, F.J.G. Silva, M.F. Andrade, R. Alexandre, A.P.M. Baptista; Increasing the lifespan of high-pressure die cast molds subjected to severe wear; *Surface & Coatings Technology* 332 (2017) 319–331
- [9] R. Shivpuri, Y.-L. Chu, K. Venkatesan, J.R. Conrad, K. Sridharan, M. Shamim, R.P. Fetherston; An evaluation of metallic coating for erosive wear resistance in die casting applications; *Wear* 192 (1996)
- [10] Phạm Lê Dân, Đặng Quốc Phú; Cơ sở kỹ thuật nhiệt; NXB Giáo dục Việt Nam, 2010
- [11] <http://matweb.com>
- [12] Alastair Long, David Thornhill, Cecil Armstrong, David Watson; Predicting die life from die temperature for high pressure dies casting aluminium alloy; *Applied Thermal Engineering* 44 (2012), 100–107
- [13] Matevž Fazarinc, Tadej Muhič, Goran Kugler, Milan Terčelj; Thermal fatigue properties of differently constructed functionally graded materials aimed for refurbishing of pressure-die-casting dies; *Engineering Failure Analysis* 25 (2012) 238–249